JACS
JOURNAL OF THE AMERICAN CHEMICAL SOCIETY

Communication

pubs.acs.org/JACS

Controlled Intercalation and Chemical Exfoliation of Layered Metal–Organic Frameworks Using a Chemically Labile Intercalating Agent

Yanjun Ding,[†] Ying-Pin Chen,[‖] Xinlei Zhang,[†] Liang Chen,[†] Zhaohui Dong,[§] Hai-Long Jiang,*[,†,‡] Hangxun Xu,*[,†] and Hong-Cai Zhou*[,‖]

[†]Department of Polymer Science and Engineering, CAS Key Laboratory of Soft Matter Chemistry, University of Science and Technology of China, Hefei, Anhui 230026, China

[‡]Department of Chemistry, Hefei National Laboratory for Physical Sciences at the Microscale, University of Science and Technology of China, Hefei, Anhui 230026, China

[§]Shanghai Synchrotron Radiation Facility, Shanghai Institute of Applied Physics, Shanghai 201800, China

[‖]Department of Materials Science and Engineering, Texas A&M University, College Station, Texas 77840, United States

Supporting Information

ABSTRACT: Creating ordered two-dimensional (2D) metal–organic framework (MOF) nanosheets has attracted extensive interest. However, it still remains a great challenge to synthesize ultrathin 2D MOF nanosheets with controlled thickness in high yields. In this work, we demonstrate a novel intercalation and chemical exfoliation approach to obtain MOF nanosheets from intrinsically layered MOF crystals. This approach involves two steps: first, layered porphyrinic MOF crystals are intercalated with 4,4′-dipyridyl disulfide through coordination bonding with the metal nodes; subsequently, selective cleavage of the disulfide bond induces exfoliation of the intercalated MOF crystals, leading to individual freestanding MOF nanosheets. This chemical exfoliation process can proceed efficiently at room temperature to produce ultrathin (~1 nm) 2D MOF nanosheets in ~57% overall yield. The obtained ultrathin nanosheets exhibit efficient and far superior heterogeneous photocatalysis performance compared with the corresponding bulk MOF.

Two-dimensional (2D) nanomaterials with atomic or molecular thickness have received broad interest in recent years because of their unique dimension-related properties and promising applications in energy storage, separation, catalysis, and nanoelectronics.[1] Recently, 2D metal–organic framework (MOF) nanosheets have emerged as a new class of 2D nanomaterials for molecular sieving, sensing, and catalysis.[2] Highly ordered ultrathin MOF nanosheets formed via coordination bonding require precise control of structure and functionality over extended length scales. MOF nanosheets are of significant importance not only for fundamental structure–property investigations but also for technological developments.[3] Nonetheless, the rational synthesis of MOF nanosheets with diverse structures and tailored properties while keeping them down to atomic thickness is still a great challenge.

The top-down method has been demonstrated to be a formidable approach for efficient and scalable production of various 2D nanomaterials.[4] Exfoliation of 3D layered MOFs into their 2D constituents is very attractive if appropriate exfoliation methods can be developed. For example, layered MOFs are diverse sources of ultrathin crystalline nanosheets for molecular sieving if they can be efficiently exfoliated while retaining their structure and morphology.[2c,d] Recent studies on exfoliation of MOFs exclusively focus on exfoliating 2D frameworks held together by interlayer van der Waals interactions or hydrogen bonding in bulk crystals.[5] Insufficient control over the mechanical or solvent-mediated exfoliation process by weakening of interlayer interactions in MOF crystals often leads to 2D nanosheets with various thicknesses and low yields (typically <15%).[2e,5f] To circumvent this problem, a more reliable exfoliation route using controllable chemical reactions to regulate the interlayer interactions is highly desired. Exfoliation of chemically preintercalated layered inorganic solids is an efficient method to synthesize ultrathin 2D inorganic nanosheets.[6] Unfortunately, the chemical intercalation method generally used for inorganic solids is not applicable to exfoliating MOFs into 2D nanosheets.

Here, for the first time, we demonstrate a new strategy for the high-yield synthesis of 2D MOF nanosheets via chemical exfoliation from intercalated MOF crystals. The overall fabrication process is schematically illustrated in Figure 1. In order to obtain chemically responsive MOFs, we incorporate a chemically labile dipyridyl ligand, 4,4′-dipyridyl disulfide (DPDS), into the layered MOF crystals to form new intercalated MOFs. Because the interlayer interactions between

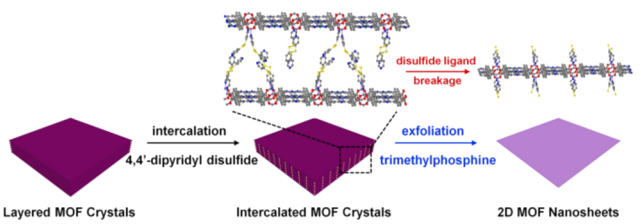

Figure 1. Schematic illustration of the overall process developed to produce 2D MOF nanosheets via an intercalation and chemical exfoliation approach.

Received: May 10, 2017
Published: June 27, 2017

DOI: 10.1021/jacs.7b04829
J. Am. Chem. Soc. 2017, 139, 9136–9139

expanded 2D layers are weakened after scissoring of DPDS by chemical reduction of the disulfide bond using trimethylphosphine (TMP), MOFs can be easily exfoliated into ultrathin (~1 nm) nanosheets in high yield (~57%). Furthermore, we demonstrate that the as-prepared nanosheets exhibit very high efficiency in singlet oxygen ($^1O_2$) generation for heterogeneous photocatalysis.

Tetrakis(4-carboxyphenyl)porphyrin (TCPP) is an extensively used organic linker to construct a variety of 2D and 3D MOFs.[7] Thus, a known MOF (PPF-1) containing porphyrin sheets with Zn dinuclear paddlewheel secondary building units (SBUs) was initially used here.[8a] The 2D layers can be inserted in the third dimension by coordination of the metal centers within the paddlewheels and inside the porphyrin rings.[8] As a result, the pyridyl ligands can be inserted into the interlayers to form a new crystal (Figure S1). Unfortunately, the diffractions were too weak for the overall structure to be determined. We then tried other metallo-TCPP (M-TCPP) species (M = Pd, Ni, Co) and obtained stronger-diffraction crystals when PdTCPP was used (Figures S2 and S3 and Table S1). Therefore, the MOF containing PdTCPP was used as a model structure for this proof-of-concept study.

As shown in Figure 2, the corresponding unit cell parameter (*c*, perpendicular to the porphyrin planes) increased from

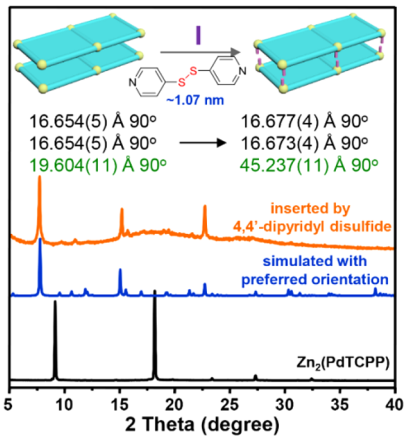

Figure 2. Experimental PXRD patterns of Zn_2(PdTCPP) before and after insertion of DPDS along with simulated results considering the preferred orientation in the (001) direction. The unit cell parameters were obtained from single-crystal X-ray crystallography.

19.604 to 45.237 Å after intercalation, indicating that the interlayer distance varied from 9.8 to 22.6 Å, which is larger than the longitudinal length of the DPDS ligand (~10 Å). This observation indicates that only one pyridinic N from each DPDS ligand coordinates to Zn from a $Zn_2(COO)_4$ SBU and that the other N is not coordinated. From the structure solved from single-crystal data for the intercalated MOF, Zn_2(PdTCPP)$(DPDS)_2$ (Figure S4 and Table S1), the PdTCPP layers are clearly observed whereas the inserted DPDS linkers are incomplete because of the random orientation of the linkers caused by free rotation of single bonds.[7d] However, X-ray photoelectron spectroscopy (XPS) (Figure S5), elemental analysis, mass spectra (Figure S6), and energy-dispersive X-ray spectroscopy (EDX) (Figure S7) results indicate the presence of DPDS in the crystals. Powder X-ray diffraction (PXRD) patterns (Figure S8) further agree that the DPDS ligands must be coordinated to the unsaturated Zn sites instead of flowing in the layers. The structure was therefore confirmed by using a similar ligand, 4-(phenyldithio)-pyridine (PDTP), in place of DPDS for the intercalation reaction (Figure S9). Moreover, the ^{1}H NMR spectrum of the digested MOF crystals shows a 1:2 ratio between PdTCPP and DPDS (Figure S10), which is consistent with the theoretical value. After intercalation, the MOF crystals retained the layered structure (Figure S11). Taking the preferred orientation into consideration,[2e,9] the experimental PXRD pattern coincides with the pattern simulated from the structure solved with single-crystal XRD data (Figure 2). The proposed structure describing coordinated DPDS ligands (Figure S12) was further verified using synchrotron-based PXRD (Figure S13). Thus, our results indicate that DPDS can be intercalated into the layered MOF crystals to form new MOF crystals with an expanded interlayer distance.[8]

The disulfide intercalating reagent, DPDS, has an absorption peak at 245 nm (Figure S14). After reduction by TMP, a new peak at 341 nm corresponding to 4-mercaptopyridine appears, suggesting that the DPDS is chemically scissored into 4-mercaptopyridine. Subsequently, after addition of TMP into an ethanol solution containing Zn_2(PdTCPP)$(DPDS)_2$ crystals, new peaks at 341 and 425 nm corresponding to 4-mercaptopyridine and PdTCPP appear (Figure 3a), implying

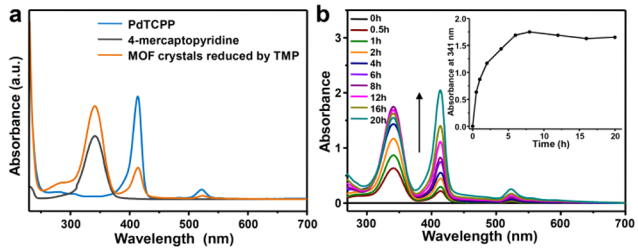

Figure 3. (a) UV–vis absorption spectra of PdTCPP, 4-mercaptopyridine, and the intercalated MOF crystals after reduction by TMP. (b) Time-course measurement of the exfoliation process by UV–vis absorption spectroscopy. Inset: the absorbance at 341 nm as a function of exfoliation time.

that the dipyridyl intercalating agents are cleaved (Figure S15). As shown in Figure 3b, upon addition of TMP, the absorption peak at 341 nm increases, and after ~10 h, the absorption intensity reaches its maximum value. Consequently, exfoliation of the MOF crystals into ultrathin nanosheets was carried out by adding a 20-fold excess of TMP into the crystal solution at room temperature with gentle stirring. Excess TMP was used to ensure that crystals were exfoliated in the highest yield. The exfoliation process occurred immediately and was evidenced by the Tyndall effect upon irradiation with a laser beam (Figure 4a, inset). The exfoliated nanosheets were characterized by transmission electron microscopy (TEM) and atomic force microscopy (AFM) (Figure 4). Both characterization methods indicated that freestanding nanosheets with sizes of up to micrometers were obtained after exfoliation (Figure S16a). Wrinkled or ruptured sheets were observed from TEM (Figure 4a,b), suggesting the ultrathin nature of the exfoliated nanosheets. As shown in Figures 4c and S16b, the height of as-exfoliated nanosheets was measured to be ~1.0 nm with slight variations, roughly corresponding to the thickness of single-layer PdTCPP nanosheets (Figure S12).

The reduction of disulfide bonds is a chemical reaction that can be quantitatively controlled by varying the amount of TMP used along with the reaction time. Generally, in order to

DOI: 10.1021/jacs.7b04829
J. Am. Chem. Soc. 2017, 139, 9136–9139

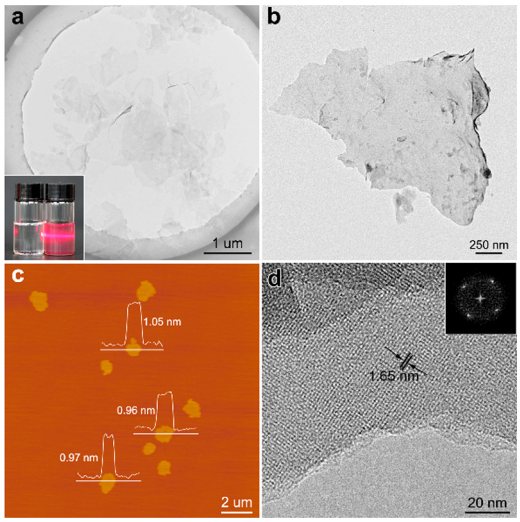

Figure 4. (a) TEM image of the exfoliated MOF nanosheets. Inset: Tyndall effect (left) before and (right) after exfoliation. (b) TEM image of an individual exfoliated MOF nanosheet. (c) AFM image of the exfoliated MOF nanosheets with corresponding height profiles. (d) High-resolution TEM image of an exfoliated multilayer MOF nanosheet. The corresponding FFT pattern is shown in the inset.

exfoliate MOF crystals into 2D nanosheets as much as possible, excess TMP was required. However, when the reaction time was shortened to 4 h and the amount of TMP used was 10-fold higher than that of the disulfide groups present in the crystals, the majority of the obtained products were multilayer nanosheets with heights of ~4 nm (Figure S17), indicating a controllable exfoliation process. More importantly, high-resolution TEM (HRTEM) clearly showed the lattice fringes of the exfoliated multilayer MOF nanosheets with an interplanar distance of 1.65 nm, which belongs to the (100) plane of the intercalated crystals (Table S1). Meanwhile, the corresponding fast Fourier transform (FFT) image also displays fourfold symmetry (Figure 4d). These results directly prove that the crystalline structure was still maintained after exfoliation. Thus, our results show that cleavage of DPDS can efficiently lead to the formation of ultrathin MOF nanosheets from intercalated MOFs. Control experiments involving addition of TMP or 4-mercaptopyridine to the Zn_2(PdTCPP) crystals did not lead to the spontaneous exfoliation process (Figure S18), confirming that exfoliation starts with the reduction of DPDS ligands. The exfoliation is likely caused by the significantly decreased interlayer interactions after removal of part of the intercalating agent, an extraction process similar to the synthesis of MXenes.[6d]

Recently, the Zhang group reported a novel surfactant-assisted synthetic method to prepare ultrathin 2D MOF nanosheets in high yields.[2e] This method can conveniently produce multilayer nanosheets (<10 nm), but it is difficult to achieve single-layer nanosheets. Moreover, a liquid exfoliation method was used to exfoliate layered Zn_2(PdTCPP) crystals for comparison. Although irregular nanosheets with thicknesses in the range of 1.5−3.5 nm could be obtained, the majority of the nanosheets were 30−120 nm in height (Figures S19 and S20). More importantly, the overall yield was ~10% with a large portion of small fragmented pieces (Figure S20). Therefore, selective chemical exfoliation from predesigned MOFs potentially allows for efficient and controllable formation of 2D MOF nanosheets.

Ultrathin 2D nanosheets typically exhibit superior photoresponsivity and enhanced photocatalytic activity with more easily accessible reaction sites.[10] Porphyrin derivatives are widely used for $^1O_2$ generation because of their unique photochemistry and high efficiency in light harvesting.[7c,11] We thus further investigated the potential application of as-exfoliated nanosheets in $^1O_2$ generation for heterogeneous photocatalysis. 1,3-Diphenylisobenzofuran (DPBF) was used to detect the $^1O_2$ evolution upon visible-light irradiation (λ > 420 nm). As shown in Figure 5a, the absorption at 410 nm

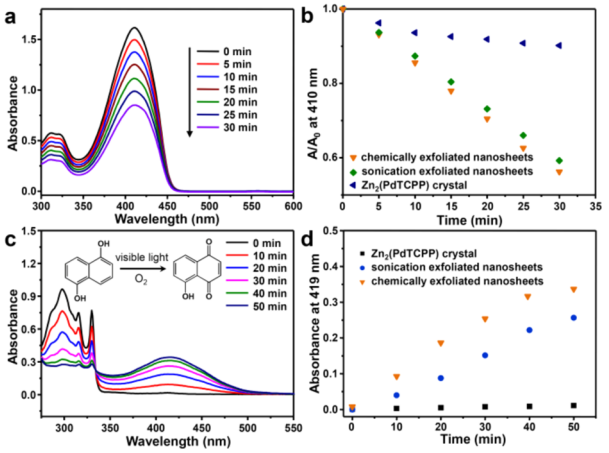

Figure 5. (a) UV−vis absorption spectra of DPBF upon visible-light irradiation in the presence of chemically exfoliated MOF nanosheets. (b) Absorbance decays of DPBF with different catalysts. (c) Photooxidation of DHN in CH_3CN catalyzed by chemically exfoliated nanosheets. (d) Absorbance of juglone (λ = 419 nm) as a function of reaction time with different catalysts.

decreases in the presence of exfoliated MOF nanosheets, indicating the formation of $^1O_2$. The chemically exfoliated nanosheets exhibit better performance in $^1O_2$ generation compared with other samples (Figure 5b). As a result, the chemically exfoliated 2D MOF nanosheets are more efficient in photooxidation of 1,5-dihydroxynaphthalene (DHN) to form the corresponding oxidized product juglone (Figure 5c,d).

In conclusion, we have successfully demonstrated a versatile approach for synthesizing 2D MOF nanosheets in high yields. This novel strategy relies on the incorporation of a chemically scissable intercalating agent, 4,4′-dipyridyl disulfide, into the intrinsically layered MOF crystals. The cleavage of intercalated disulfide groups occurs rapidly and, to a certain degree, is capable of controlling the thickness of the exfoliated MOF nanosheets. Considering the vast number of available organic ligands and metal nodes in MOFs, the approach demonstrated here holds great promise for synthesizing various ultrathin 2D metal−organic nanosheets with desired structures and properties.

■ ASSOCIATED CONTENT

Supporting Information

The Supporting Information is available free of charge on the ACS Publications website at DOI: 10.1021/jacs.7b04829.

Detailed synthesis, single-crystal data, and additional PXRD, SEM, TEM, AFM, NMR, and XPS characterization results (PDF)

Crystallographic data for Zn_2(PdTCPP) (CIF)

DOI: 10.1021/jacs.7b04829
J. Am. Chem. Soc. 2017, 139, 9136−9139

Crystallographic data for Zn_2(PdTCPP) intercalated with DPDS (CIF)

AUTHOR INFORMATION

Corresponding Authors

*(H.X.) hxu@ustc.edu.cn
*(H.L.J.) jianglab@ustc.edu.cn
*(H.C.Z.) zhou@chem.tamu.edu

ORCID

Hai-Long Jiang: 0000-0002-2975-7977
Hangxun Xu: 0000-0003-1645-9003
Hong-Cai Zhou: 0000-0002-9029-3788

Notes

The authors declare no competing financial interest.

ACKNOWLEDGMENTS

We acknowledge beamline 15U1 at Shanghai Synchrotron Radiation Facility (SSRF) for the XRD measurements. We also thank Prof. S. Wang for acquiring the single-crystal XRD data. This work was supported by the National Key Basic Research Program of China (2015CB351903 and 2014CB931803), the National Natural Science Foundation of China (51402282, 21474095, 21371162, 21673213, and 21521001), and the CAS Key Research Program of Frontier Sciences (QYZDB-SSW-SLH018). Y.-P.C. was funded by Texas A&M University. H.-C.Z. gratefully acknowledges support from the Welch Foundation (A-0030).

REFERENCES

(1) (a) Novoselov, K. S.; Fal'ko, V. I.; Colombo, L.; Gellert, P. R.; Schwab, M. G.; Kim, K. *Nature* **2012**, *490*, 192. (b) Lv, R.; Robinson, J. A.; Schaak, R. E.; Sun, D.; Sun, Y.; Mallouk, T. E.; Terrones, M. *Acc. Chem. Res.* **2015**, *48*, 56. (c) Zhang, H. *ACS Nano* **2015**, *9*, 9451. (d) Wang, H.; Yuan, H.; Hong, S. S.; Li, Y.; Cui, Y. *Chem. Soc. Rev.* **2015**, *44*, 2664.

(2) (a) Campbell, M. G.; Liu, S. F.; Swager, T. M.; Dincă, M. *J. Am. Chem. Soc.* **2015**, *137*, 13780. (b) Cao, L.; Lin, Z.; Peng, F.; Wang, W.; Huang, R.; Wang, C.; Yan, J.; Liang, J.; Zhang, Z.; Zhang, T.; Long, L.; Sun, J.; Lin, W. *Angew. Chem., Int. Ed.* **2016**, *55*, 4962. (c) Peng, Y.; Li, Y.; Ban, Y.; Jin, H.; Jiao, W.; Liu, X.; Yang, W. *Science* **2014**, *346*, 1356. (d) Rodenas, T.; Luz, I.; Prieto, G.; Seoane, B.; Miro, H.; Corma, A.; Kapteijn, F.; Llabres i Xamena, F. X.; Gascon, J. *Nat. Mater.* **2015**, *14*, 48. (e) Zhao, M.; Wang, Y.; Ma, Q.; Huang, Y.; Zhang, X.; Ping, J.; Zhang, Z.; Lu, Q.; Yu, Y.; Xu, H.; Zhao, Y.; Zhang, H. *Adv. Mater.* **2015**, *27*, 7372.

(3) (a) Makiura, R.; Motoyama, S.; Umemura, Y.; Yamanaka, H.; Sakata, O.; Kitagawa, H. *Nat. Mater.* **2010**, *9*, 565. (b) Tan, J. C.; Saines, P. J.; Bithell, E. G.; Cheetham, A. K. *ACS Nano* **2012**, *6*, 615. (c) Zhao, M.; Lu, Q.; Ma, Q.; Zhang, H. *Small Methods* **2017**, *1*, 1600030.

(4) (a) Naguib, M.; Gogotsi, Y. *Acc. Chem. Res.* **2015**, *48*, 128. (b) Niu, L.; Coleman, J. N.; Zhang, H.; Shin, H.; Chhowalla, M.; Zheng, Z. *Small* **2016**, *12*, 272. (c) Park, S.; Ruoff, R. S. *Nat. Nanotechnol.* **2009**, *4*, 217.

(5) (a) Cao, F.; Zhao, M.; Yu, Y.; Chen, B.; Huang, Y.; Yang, J.; Cao, X.; Lu, Q.; Zhang, X.; Zhang, Z.; Tan, C.; Zhang, H. *J. Am. Chem. Soc.* **2016**, *138*, 6924. (b) Hermosa, C.; Horrocks, B. R.; Martínez, J. I.; Liscio, F.; Gómez-Herrero, J.; Zamora, F. *Chem. Sci.* **2015**, *6*, 2553. (c) Foster, J. A.; Henke, S.; Schneemann, A.; Fischer, R. A.; Cheetham, A. K. *Chem. Commun.* **2016**, *52*, 10474. (d) Junggeburth, S. C.; Diehl, L.; Werner, S.; Duppel, V.; Sigle, W.; Lotsch, B. V. *J. Am. Chem. Soc.* **2013**, *135*, 6157. (e) Gallego, A.; Hermosa, C.; Castillo, O.; Berlanga, I.; Gómez-García, C. J.; Mateo-Martí, E.; Martínez, J. I.; Flores, F.; Gómez-Navarro, C.; Gómez-Herrero, J.; Delgado, S.; Zamora, F. *Adv. Mater.* **2013**, *25*, 2141. (f) Li, P. Z.; Maeda, Y.; Xu, Q. *Chem. Commun.* **2011**, *47*, 8436. (g) Zhao, S. L.; Wang, Y.; Dong, J. C.; He, C. T.; Yin, H. J.; An, P. F.; Zhao, K.; Zhang, X. F.; Gao, C.; Zhang, L. J.; Lv, J. W.; Wang, J. X.; Zhang, J. Q.; Khattak, A. M.; Khan, N. A.; Wei, Z. X.; Zhang, J.; Liu, S. Q.; Zhao, H. J.; Tang, Z. Y. *Nat. Energy* **2016**, *1*, 16184.

(6) (a) Zheng, J.; Zhang, H.; Dong, S.; Liu, Y.; Nai, C. T.; Shin, H. S.; Jeong, H. Y.; Liu, B.; Loh, K. P. *Nat. Commun.* **2014**, *5*, 2995. (b) Huang, X.; Zeng, Z.; Zhang, H. *Chem. Soc. Rev.* **2013**, *42*, 1934. (c) Ma, R.; Sasaki, T. *Acc. Chem. Res.* **2015**, *48*, 136. (d) Naguib, M.; Gogotsi, Y. *Acc. Chem. Res.* **2015**, *48*, 128.

(7) (a) Gao, W. Y.; Chrzanowski, M.; Ma, S. *Chem. Soc. Rev.* **2014**, *43*, 5841. (b) Morris, W.; Volosskiy, B.; Demir, S.; Gándara, F.; McGrier, P. L.; Furukawa, H.; Cascio, D.; Stoddart, J. F.; Yaghi, O. M. *Inorg. Chem.* **2012**, *51*, 6443. (c) Son, H. J.; Jin, S.; Patwardhan, S.; Wezenberg, S. J.; Jeong, N. C.; So, M.; Wilmer, C. E.; Sarjeant, A. A.; Schatz, G. C.; Snurr, R. Q.; Farha, O. K.; Wiederrecht, G. P.; Hupp, J. T. *J. Am. Chem. Soc.* **2013**, *135*, 862. (d) Park, J.; Feng, D.; Yuan, S.; Zhou, H. C. *Angew. Chem., Int. Ed.* **2015**, *54*, 430.

(8) (a) Burnett, B. J.; Choe, W. *CrystEngComm* **2012**, *14*, 6129. (b) Burnett, B. J.; Barron, P. M.; Hu, C.; Choe, W. *J. Am. Chem. Soc.* **2011**, *133*, 9984. (c) Karagiaridi, O.; Bury, W.; Mondloch, J. E.; Hupp, J. T.; Farha, O. K. *Angew. Chem., Int. Ed.* **2014**, *53*, 4530. (d) Li, T.; Kozlowski, M. T.; Doud, E. A.; Blakely, M. N.; Rosi, N. L. *J. Am. Chem. Soc.* **2013**, *135*, 11688.

(9) Choi, E. Y.; Barron, P. M.; Novotny, R. W.; Son, H. T.; Hu, C. H.; Choe, W. *Inorg. Chem.* **2009**, *48*, 426.

(10) (a) Wang, H.; Yang, X.; Shao, W.; Chen, S.; Xie, J.; Zhang, X.; Wang, J.; Xie, Y. *J. Am. Chem. Soc.* **2015**, *137*, 11376. (b) Yang, S.; Gong, Y.; Zhang, J.; Zhan, L.; Ma, L.; Fang, Z.; Vajtai, R.; Wang, X.; Ajayan, P. M. *Adv. Mater.* **2013**, *25*, 2452.

(11) (a) DeRosa, M. C.; Crutchley, R. J. *Coord. Chem. Rev.* **2002**, *233–234*, 351. (b) Chen, Y. Z.; Wang, Z. U.; Wang, H.; Lu, J.; Yu, S. H.; Jiang, H. L. *J. Am. Chem. Soc.* **2017**, *139*, 2035.

DOI: 10.1021/jacs.7b04829
J. Am. Chem. Soc. 2017, 139, 9136–9139